Reprinted from LANGMUIR, 1992, 8.

Self-Assembled Monolayers of Alkanethiols on Gold: Comparisons of Monolayers Containing Mixtures of Short- and Long-Chain Constituents with CH_3 and CH_2OH Terminal Groups[1]

John P. Folkers,[2] Paul E. Laibinis, and George M. Whitesides*

Department of Chemistry, Harvard University, Cambridge, Massachusetts 02138

Received February 28, 1992

This paper describes the preparation and properties of self-assembled monolayers (SAMs) obtained by the competitive adsorption of short-chain and long-chain alkanethiols onto evaporated gold. Four systems were studied involving combinations of one short and one long chain: $HS(CH_2)_{10}CH_3$ (Sh = CH_3), $HS(CH_2)_{10}CH_2OH$ (Sh = CH_2OH), $HS(CH_2)_{21}CH_3$ (Lg = CH_3), and $HS(CH_2)_{21}CH_2OH$ (Lg = CH_2OH). The combinations examined were Sh = CH_3/Lg = CH_3, Sh = CH_3/Lg = CH_2OH, Sh = CH_2OH/Lg = CH_3, and Sh = CH_2OH/Lg = CH_2OH. The resulting monolayers were characterized by ellipsometry, X-ray photoelectron spectroscopy (XPS), and wettability by water and hexadecane. Because the two components in each SAM have different chain lengths, the thickness of a two-component SAM (as determined by ellipsometry) could be used to determine the relative amounts of each in the SAM. Intensities of XPS signals could also be used to measure the composition of the SAMs. Comparisons of compositions inferred from ellipsometry and XPS indicate that, although the two methods give results in excellent agreement, the XPS method has the higher precision and is generally superior for these types of SAMs. Comparison of the composition of the SAMs with the composition of the solutions from which they were formed suggests the order of stabilities of pairs of alkyl groups in the SAMs is long–long > short–short > long–short. This result suggests that these monolayers phase separate to some extent into microscopic islands; studies of wetting suggest that the phase separation is not complete.

Introduction

Organic thiols adsorb onto gold surfaces from solution and form ordered monolayers (self-assembled monolayers, SAMs).[3-15] By using solutions containing two different alkanethiols, it is possible to form SAMs containing mixtures of them (as the corresponding thiolates).[15-26] If the two alkanethiols ($HS(CH_2)_{sh}Sh$ and $HS(CH_2)_{lg}Lg$; Sh and Lg are the terminal functional groups) differ in the length of their chains (sh = short; lg = long), the two-component or "mixed" SAMs can be considered in terms of two regions in the direction normal to the surface of the gold (Figure 1):[21] a highly ordered hydrocarbon region near the gold–monolayer interface consisting of the methylene groups of the shorter chain thiol and the corresponding sections of the longer chain thiol (region 1 in Figure 1) and a region farther from the gold—corresponding to the remainder of the longer chains (region 2 in Figure 1)—whose order depends on the ratio of concentrations of species in the SAM (R_{SAM}, eq 2), on the difference in

$$R_{soln} = \frac{[HS(CH_2)_{lg}Lg]_{soln}}{[HS(CH_2)_{sh}Sh]_{soln}} \quad (1)$$

$$R_{SAM} = \frac{[Au/S(CH_2)_{lg}Lg]_{SAM}}{[Au/S(CH_2)_{sh}Sh]_{SAM}} \quad (2)$$

the lengths (lg − sh) of the polymethylene chains, and on the degree of homogeneity in mixing of the two components in the plane of the monolayer. It is possible to control the

(1) This research was supported in part by the Office of Naval Research, the Defense Advanced Research Projects Agency. XPS spectra were obtained using instrument facilities purchased under the DARPA/URI program and maintained by the Harvard University Materials Research Laboratory.
(2) NIH pre-doctoral trainee in biophysics, 1989–1990.
(3) Nuzzo, R. G.; Allara, D. L. *J. Am. Chem. Soc.* **1983**, *105*, 4481–4483.
(4) Porter, M. D.; Bright, T. B.; Allara, D. L.; Chidsey, C. E. D. *J. Am. Chem. Soc.* **1987**, *109*, 3559–3568.
(5) Bain, C. D.; Troughton, E. B.; Tao, Y.-T.; Evall, J.; Whitesides, G. M. *J. Am. Chem. Soc.* **1989**, *111*, 321–335.
(6) Strong, L.; Whitesides, G. M. *Langmuir* **1988**, *4*, 546–558.
(7) Chidsey, C. E. D.; Liu, G.-Y.; Rowntree, P.; Scoles, G. *J. Chem. Phys.* **1989**, *91*, 4421–4423.
(8) Hautman, J.; Klein, M. L. *J. Chem. Phys.* **1989**, *91*, 4994–5001.
(9) Ulman, A.; Eilers, J. E.; Tillman, N. *Langmuir* **1989**, *5*, 1147–1152.
(10) Nuzzo, R. G.; Dubois, L. H.; Allara, D. L. *J. Am. Chem. Soc.* **1990**, *112*, 558–569.
(11) Nuzzo, R. G.; Korenic, E. M.; Dubois, L. H. *J. Chem. Phys.* **1990**, *93*, 767–773.
(12) Chidsey, C. E. D.; Loiacono, D. N. *Langmuir* **1990**, *6*, 682–691.
(13) Widrig, C. A.; Alves, C. A.; Porter, M. D. *J. Am. Chem. Soc.* **1991**, *113*, 2805–2810.
(14) Laibinis, P. E.; Whitesides, G. M.; Allara, D. L.; Tao, Y.-T.; Parikh, A. N.; Nuzzo, R. G. *J. Am. Chem. Soc.* **1991**, *113*, 7152–7167.
(15) For reviews, see: Bain, C. D.; Whitesides, G. M. *Angew. Chem., Int. Ed. Engl.* **1989**, *28*, 506–512. Whitesides, G. M.; Laibinis, P. E. *Langmuir* **1990**, *6*, 87–96. Ulman, A. *An Introduction to Ultrathin Organic Films from Langmuir-Blodgett to Self-Assembly*; Academic Press: San Diego, CA, 1991; Chapter 3.
(16) Bain, C. D.; Whitesides, G. M. *J. Am. Chem. Soc.* **1988**, *110*, 6560–6561.
(17) Bain, C. D.; Evall, J.; Whitesides, G. M. *J. Am. Chem. Soc.* **1989**, *111*, 7155–7164.
(18) Bain, C. D.; Whitesides, G. M. *J. Am. Chem. Soc.* **1988**, *110*, 3665–3666.
(19) Bain, C. D.; Whitesides, G. M. *Science (Washington, D.C.)* **1988**, *240*, 62–63.
(20) Bain, C. D.; Whitesides, G. M. *J. Am. Chem. Soc.* **1989**, *111*, 7164–7175.
(21) Laibinis, P. E.; Nuzzo, R. G.; Whitesides, G. M. *J. Phys. Chem.*, in press.
(22) Pale-Grosdemange, C.; Simon, E. S.; Prime, K. L.; Whitesides, G. M. *J. Am. Chem. Soc.* **1991**, *113*, 12–20. Prime, K. L.; Whitesides, G. M. *Science (Washington, D.C.)* **1991**, *252*, 1164–1167.
(23) Ulman, A.; Evans, S. D.; Shnidman, Y.; Sharma, R.; Eilers, J. E.; Chang, J. C. *J. Am. Chem. Soc.* **1991**, *113*, 1499–1506.
(24) Laibinis, P. E.; Whitesides, G. M. *J. Am. Chem. Soc.* **1992**, *114*, 1990–1995.
(25) Chidsey, C. E. D.; Bertozzi, C. R.; Putvinski, T. M.; Mujsce, A. M. *J. Am. Chem. Soc.* **1990**, *112*, 4301–4306.
(26) Collard, D. M.; Fox, M. A. *Langmuir* **1991**, *7*, 1192–1197.

0743-7463/92/2408-1330$03.00/0

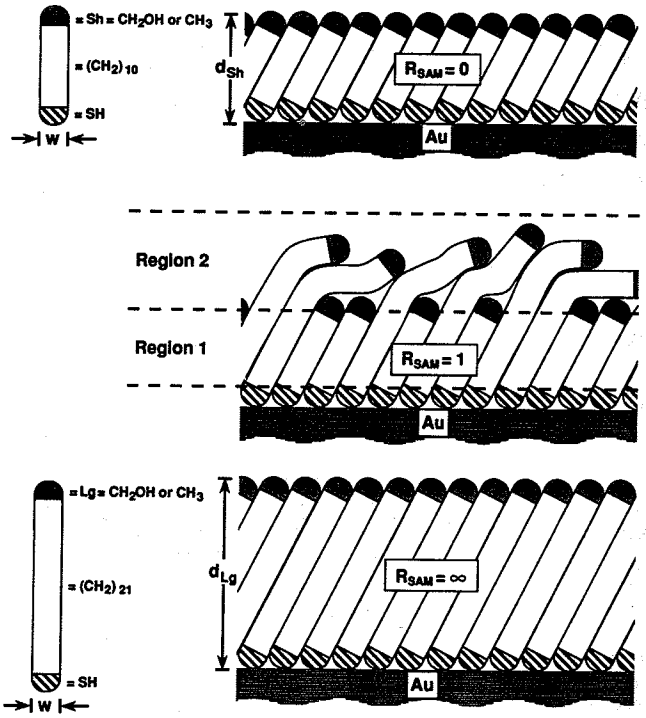

Figure 1. Schematic representations of monolayers with $R_{SAM} = 0$ (top), $R_{SAM} = 1$ (middle), and $R_{SAM} = \infty$ (bottom). R_{SAM} is defined by eq 2. The mixed SAM has the two components well mixed for illustrative purposes only. The width of the hydrocarbon chain (w) is 4.5 Å,[14] the thickness of a SAM of the shorter component (d_{Sh}) is approximately 14 Å (as measured using ellipsometry), and the thickness of a SAM of the longer component (d_{Lg}) is approximately 28 Å. See the text for definitions of the two regions in the mixed SAM.

properties of the mixed SAMs by controlling the value of R_{SAM}, the number of outer methylene groups lg–sh, and the tail groups Sh and Lg.[18-22]

In general, the ratio of the concentrations of the two thiols in solution (R_{soln}, eq 1) does not equal the ratio of the thiolates derived from them in the SAM (eq 2),[16-22,24] and we cannot predict quantitatively the value of R_{soln} that will yield a SAM with a desired value of R_{SAM}. The procedure we have adopted in studying mixed SAMs is to prepare SAMs from solutions spanning the complete range of R_{soln}, to examine their ellipsometric thicknesses, X-ray photoelectron spectra, and wettabilities as a function of R_{soln}, and to infer values of R_{SAM} from this information.

The experimental conditions used in this study generate SAMs with compositions that are, at least in part, kinetically determined.[27] That is, the mixture of thiolates in the SAM is not in complete thermodynamic equilibrium with the mixture of thiols in solution. Defining the important reactions that determine the composition and structure of the SAMs (adsorption and desorption of the thiols, thiolates, and disulfides to/from the different regions on the gold surface; phase separation on the surface) is a complex problem that we will address in future papers.[27] The conditions we have used here (samples immersed in ethanolic solutions containing a total concentration of thiol of 1 mM for 1 day at room temperature) are representative of those used in most of the published work based on two-component SAMs derived from alkanethiols,[16-22,24-26] but with these components, the composition of the SAMs is neither kinetic nor thermodynamic.

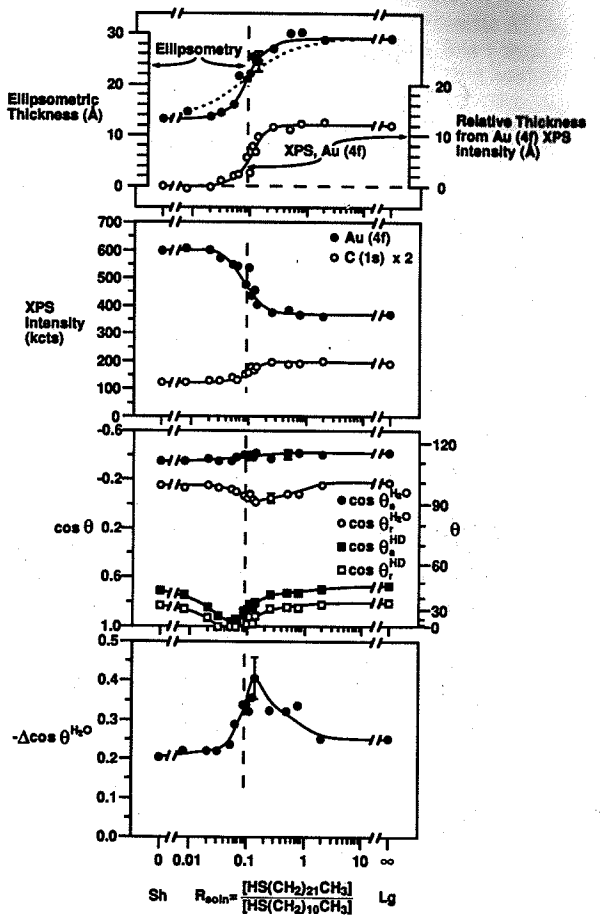

Figure 2. Ellipsometric, XPS, and wetting data for SAMs on gold formed by exposure of freshly evaporated gold substrates to mixtures of $HS(CH_2)_{21}CH_3$ and $HS(CH_2)_{10}CH_3$ in ethanol for 1 day at room temperature. In the top plot, filled circles represent the thickness of the SAMs determined by ellipsometry; open circles represent the thickness of the SAMs relative to the thickness of the shorter component, determined from the Au(4f) intensity (see eqs 13 and 15). XPS intensities are given in units of thousands of counts ("kilocounts"). Increasing values of hysteresis in the contact angle of water (bottom plot) correspond to larger values of $(\cos \theta_a^{H_2O} - \cos \theta_r^{H_2O})$. Solid lines through the data are provided as guides to the eye. The vertical dashed line represents the value of R_{soln} that leads to $R_{SAM} = 1$ as determined by ellipsometry. The dashed curve through the data of ellipsometric thickness was determined using eq 12 and the assumptions in eqs 5–7: It represents the expected form of the data if the thiolates in the SAM were in thermodynamic equilibrium with thiols in solution, and mixing between components was ideal. The error bar indicated in the plot ellipsometric thicknesses is representative of the observed precision for thicknesses of SAMs of alkanethiolates on gold (±2 Å). Error bars on XPS measurements could not be determined, but we estimate fluctuations in the intensity of the X-ray source to be less than 5%. Error bars on data for contact angles of water represent the average error bar for the contact angles in the transition region. Error bars on data for contact angles of hexadecane are smaller than the size of the symbols. The error in hysteresis was determined from the average error in $\cos \theta_a^{H_2O}$ and $\cos \theta_r^{H_2O}$. Specific details concerning the determination of error bars are given in footnotes in the text.

The purpose of this work was to provide directly comparable sets of data for competitive adsorption experiments for four possible combinations of end groups for sh = 10, lg = 21: Sh = CH_3/Lg = CH_3, Sh = CH_3/Lg = CH_2OH, Sh = CH_2OH/Lg = CH_3, and Sh = CH_2OH/Lg = CH_2OH.[28] We have previously described several of these

(27) In a separate paper we will describe the kinetics and thermodynamics of formation of these mixed SAMs, as well as studies of the effects of time, temperature, and total concentration of thiols on the composition of the SAMs. In these studies we will also define the conditions necessary to generate SAMs closer to equilibrium than those described in this paper and discuss the properties of these SAMs.

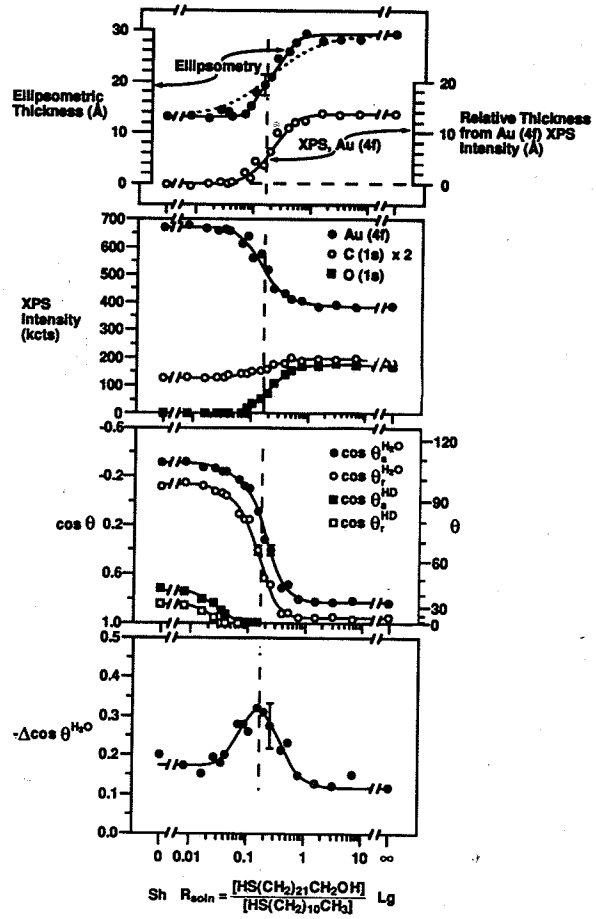

Figure 3. Ellipsometric, XPS, and wetting data for SAMs on gold formed from exposure of freshly evaporated gold substrates to mixtures of $HS(CH_2)_{21}CH_2OH$ and $HS(CH_2)_{10}CH_3$ in ethanol for 1 day at room temperature. Descriptions of the plots are given in the caption to Figure 2.

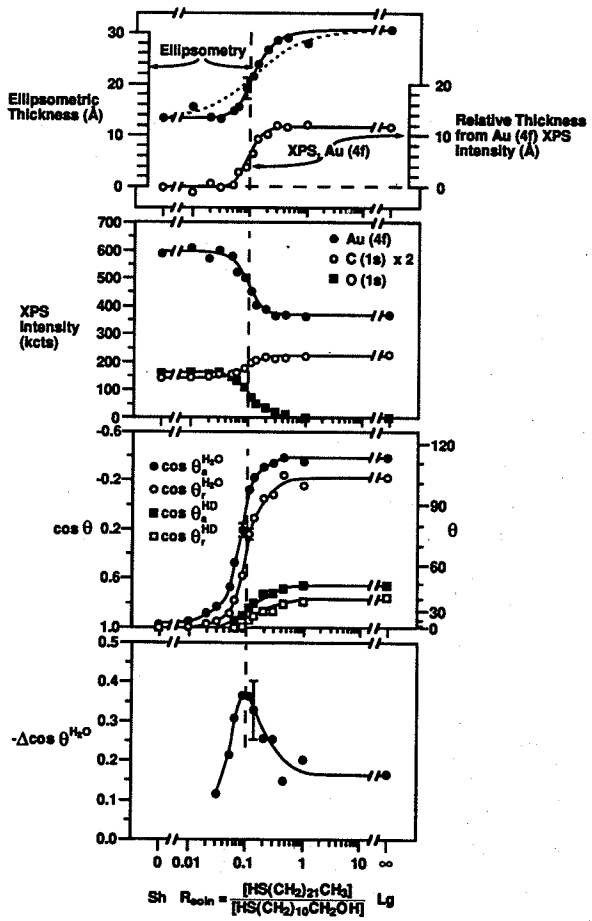

Figure 4. Ellipsometric, XPS, and wetting data for SAMs on gold formed from exposure of freshly evaporated gold substrates to mixtures of $HS(CH_2)_{21}CH_3$ and $HS(CH_2)_{10}CH_2OH$ in ethanol for 1 day at room temperature. Descriptions of the plots are given in the caption to Figure 2.

systems individually,[18-20] but the sets of data were not comparable. We wished to have a complete, carefully collected set of data for a representative set of components incorporated into mixed SAMs, in order to define trends and phenomena of interest and to have reference data against which to compare other studies. We chose methyl and hydroxymethyl groups as the terminal functional groups to give a large difference in the wetting properties of the resulting SAMs and to enable the terminal groups to allow estimation of the compositions of the SAMs by X-ray photoelectron spectroscopy (XPS). All four thiols are synthetically accessible or commercially available, are soluble in ethanol at millimolar concentrations, form ordered single-component SAMs whose structures and properties have been studied,[3-15] and form mixed SAMs that span a range of thickness easily characterized by ellipsometry and XPS.

We wished to answer four questions with these experiments. First, what techniques (ellipsometry, XPS, or wettability) are most reliable for determining the composition of the mixed SAMs for a given system, and how well do values obtained by different techniques agree? Second, how sensitive to the surface structure of SAMs are the values of contact angle and the hysteresis in contact angle? Third, do studies of wetting using water and hexadecane as probe liquids give different kinds of information about the structure of the mixed SAMs? Fourth, is there evidence for phase separation in these SAMs?

Results

Experimental Conditions. Figures 2–5 present data for competitive adsorption experiments conducted using a common set of experimental conditions. We emphasize again that these conditions generate SAMs that are kinetically controlled: Different conditions generate SAMs with different compositions.[27] The SAMs used to generate the data in Figures 2–5 were obtained by exposing freshly evaporated gold substrates to solutions of the thiols for 1 day at room temperature, using deoxygenated absolute ethanol as solvent. The *total* concentration of thiol in each solution was 1 mM in every experiment. Data in Figures 2–5 are plotted against R_{soln}; values of R_{SAM} must be inferred from the measured characteristics of the SAMs.

Morphology of the Gold Substrates. In Figure 6 we present a scanning electron micrograph (SEM) of a typical gold substrate. The surface is relatively featureless, but does appear to consist of small mounds on the order of 100 nm across. The scanning tunneling microscope[30] (STM) provides more detail about the morphology of these surfaces (Figure 7). This representative section of surface consists of mounds of gold approximately 70 nm across and 20–30 nm high. We present these images as a reference for comparison to later studies that will describe the effects

(28) We use these labels for consistency with a paper that compares the properties of similar mixed SAMs formed on silver to those formed on gold.[29]

(29) Laibinis, P. E.; Fox, M. A.; Folkers, J. P.; Whitesides, G. M. *Langmuir* **1991**, *7*, 3167–3173.

(30) Binnig, G.; Rohrer, H.; Gerber, C.; Weibel, E. *Phys. Rev. Lett.* **1982**, *49*, 57–61. Binnig, G.; Rohrer, H. *Angew. Chem., Int. Ed. Engl.* **1987**, *26*, 606–614.

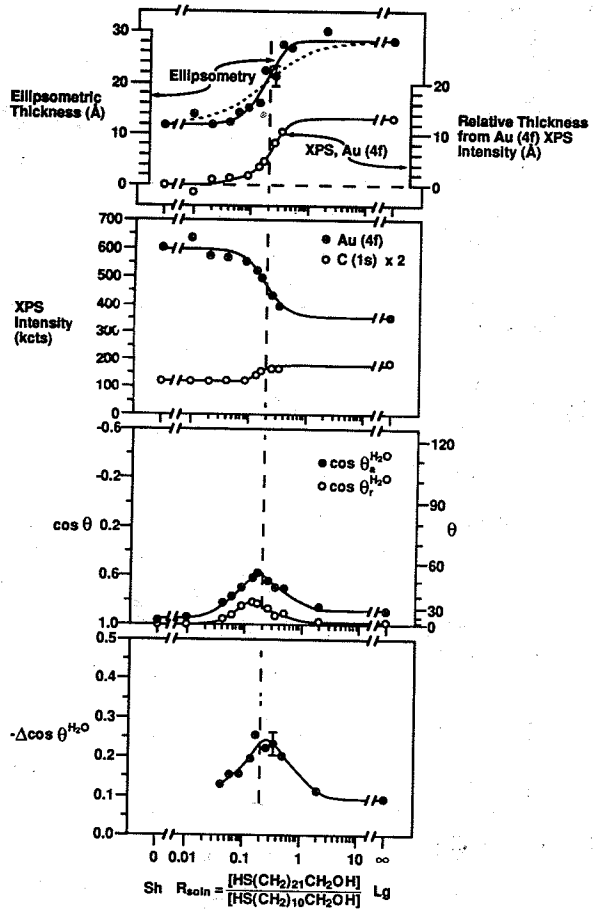

Figure 5. Ellipsometric, XPS, and wetting data for SAMs on gold formed from exposure of freshly evaporated gold substrates to mixtures of $HS(CH_2)_{21}CH_2OH$ and $HS(CH_2)_{10}CH_2OH$ in ethanol for 1 day at room temperature. Descriptions of the plots are given in the caption to Figure 2.

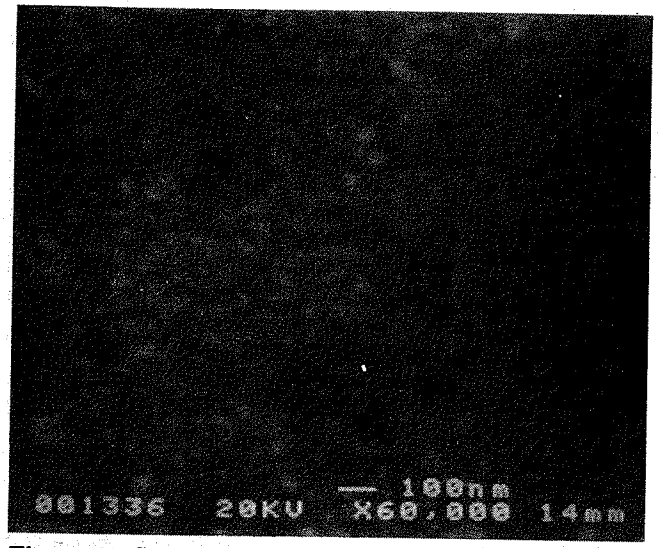

Figure 6. Scanning electron micrograph of a typical gold substrate.

of the morphology of the gold surface on the composition of mixed SAMs. Gold surfaces with large, flat terraces[31]

(31) For examples of annealing procedures and STM images of the surfaces see: Hallmark, V. M.; Chiang, S.; Rabolt, J. F.; Swalen, J. D.; Wilson, R. J. *Phys. Rev. Lett.* **1987**, *59*, 2879–2882. Chidsey, C. E. D.; Loiacono, D. N.; Sleator, T.; Nakahara, S. *Surf. Sci.* **1988**, *200*, 45–66. Emch, R.; Nogami, J.; Dovek, M. M.; Lang, C. A.; Quate, C. F. *J. Appl. Phys.* **1989**, *65*, 79–84. Putnam, A.; Blackford, B. L.; Jericho, M. H.; Watanabe, M. O. *Surf. Sci.* **1989**, *217*, 276–288. Vancea, J.; Reiss, G.; Schneider, F.; Bauer, K.; Hoffmann, H. *Surf. Sci.* **1989**, *218*, 108–126.

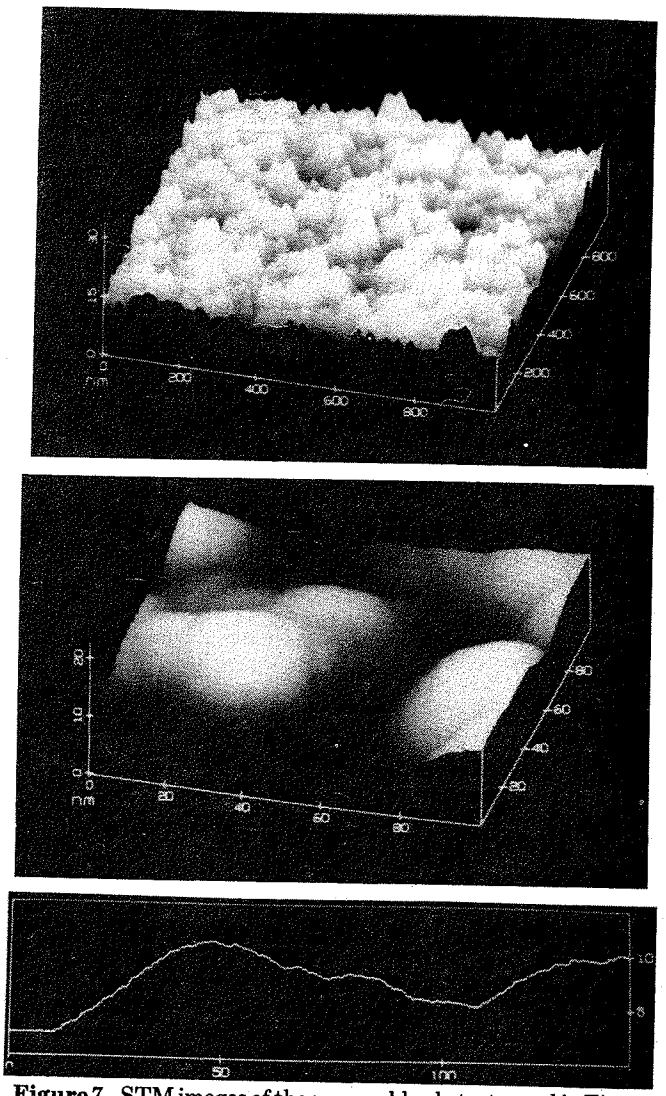

Figure 7. STM images of the same gold substrate used in Figure 6. The top image is a 1000 nm × 1000 nm region of the gold. The height scale is 30 nm. The bottom image is a 100 nm × 100 nm expansion of a part of the top image. The line topography map of this latter image was taken from the lower left-hand corner of the image to the upper right. The height scale is 10 nm.

may lead to different compositions under these experimental conditions because exchange between thiolates in a SAM and organosulfur species in solution seems to be influenced by morphological features—steps, defects, grain boundaries—in the gold surface in ways that have not so far been clearly defined.[32]

Ellipsometric Thickness. We assume that the measured ellipsometric thickness of a SAM, $d_{SAM,ellip}$, is directly related to its composition through eq 3 (χ_{Sh} and χ_{Lg} are

$$d_{SAM,ellip} = \chi_{Sh} d_{Sh,ellip} + \chi_{Lg} d_{Lg,ellip} \qquad (3)$$

the mole fractions of the individual components in the SAM, $\chi_{Sh} + \chi_{Lg} \equiv 1$; $d_{Sh,ellip}$ and $d_{Lg,ellip}$ are the ellipsometric thicknesses of the single-component SAMs). This assumption requires only that the index of refraction of the ordered and disordered regions depicted in Figure 1 be the same regardless of the value of R_{SAM}.[33] This assumption—within the experimental precision of our ellipsometer (±~2 Å for SAMs on gold)[34]—is supported by

(32) Results from several studies on the kinetics of exchange between thiols in solution and thiolates on the surface have implied that exchange is influenced or dominated by defects sites in the monolayer.[17,25,26,29]

Table I. Values of $1/R_{soln}^{SAM=1}$ Estimated from Different Properties of the Mixed SAMs[a]

	$1/R_{soln}^{SAM=1}$, estimated from:						
system	d_{SAM}	ln [C(1s)/ Au(4f)]$_{SAM}$	ln Au(4f)$_{SAM}$	O(1s)	$\cos\theta_a^{H_2O}$	$\cos\theta_r^{H_2O}$	av
Sh = CH_3/Lg = CH_3	12	11	10	–[b]	–	–	11
Sh = CH_3/Lg = CH_2OH	5	6	5	5	5	7	6
Sh = CH_2OH/Lg = CH_3	8	11	10	9	13	10	10[c]
Sh = CH_2OH/Lg = CH_2OH	6	5	5	–	–	–	5

[a] Values are unitless: they are ratios of the concentrations of the two thiols in solution that result in $R_{SAM} = 1$ (using the experimental probe of the composition of the mixed SAMs indicated in each of the column headings). [b] Dashes represent measurements that either were not taken or could not be related to R_{SAM} by an equation of the form of eq 8. [c] The average value for Sh = CH_2OH/Lg = CH_3 was determined without the value determined from the advancing contact angle of water because it is not related to the surface composition by an equation of the form of eq 8.

alternative analyses based on XPS (see below) and an independent study using radioisotopically labeled components.[35]

Using the ellipsometric thicknesses of the mixed SAMs and eq 3, we have inferred values of R_{soln} that generate SAMs having $R_{SAM} = 1$ for all four systems. The reciprocal of R_{soln} at which $R_{SAM} = 1$ ($1/R_{soln}^{SAM=1}$, eq 4; we use the reciprocal only because it is convenient to work with numbers greater than 1) is a convenient parameter to use in comparing systems (Table I).[36] This parameter gives

$$1/R_{soln}^{SAM=1} = \left\{\frac{[HS(CH_2)_{sh}/Sh]_{soln}}{[HS(CH_2)_{lg}/Lg]_{soln}}\right\}_{t,T,[Sh]+[Lg]} \quad (4)$$

the preference of the SAM for the longer chain component under these experimental conditions. Because the composition of the SAMs is influenced by kinetics, the values of $1/R_{soln}^{SAM=1}$ depend on the length of time for adsorption (t), the temperature of the adsorptions (T), and the total concentration of thiol in solution ([Sh] + [Lg]).[27]

Values of $1/R_{soln}^{SAM=1}$ can also be estimated from different experimental parameters used to characterize the SAMs—cos θ and XPS intensities—using relations analogous to eq 3 (see below).[36] Table I also list these values. The average of these values is indicated in Figures 2–5 by the dashed, vertical lines. These lines allow easy comparison between different sets of data.

Simplest Case: Independent Sites, Thermodynamic Equilibrium. To have a reference against which to compare the experimentally determined relationship between ellipsometric thickness and R_{soln}, we first assume the simplest model for self-assembly of the mixed SAMs: The two components adsorb independently on the surface, with free energies of adsorption differing by α (eq 5), and

$$\alpha = \Delta G_{ads,Lg} - \Delta G_{ads,Sh} \quad (5)$$

the adsorbed thiolates on the surface are in thermodynamic equilibrium with thiols in solution (eqs 6 and 7; $A = \exp(-\alpha/RT)$).[37] For some experimental parameter of the

$$Sh_{soln} + Sh^*_{SAM} \overset{K}{\rightleftharpoons} Sh_{SAM} + Sh^*_{soln} \quad (6)$$

$$Lg_{soln} + Lg^*_{SAM} \overset{AK}{\rightleftharpoons} Lg_{SAM} + Lg^*_{soln} \quad (7)$$

SAM (P_{SAM}) that we can assume to be related linearly to the composition of the SAM (eq 8, e.g. thickness, cos θ, elemental composition), eq 11 describes the relationship

$$P_{SAM} = \chi_{Sh}P_{Sh} + \chi_{Lg}P_{Lg} \quad (8)$$

$$P_{SAM} = P_{Sh} + \chi_{Lg}(P_{Lg} - P_{Sh}) \quad (9)$$

$$P_{SAM} = P_{Sh} + (P_{Lg} - P_{Sh})\left(\frac{R_{SAM}}{1 + R_{SAM}}\right) \quad (10)$$

$$P_{SAM} = P_{Sh} + (P_{Lg} - P_{Sh})\left(\frac{AR_{soln}}{1 + AR_{soln}}\right) \quad (11)$$

between the experimental parameters for the pure and mixed SAMs where P_{Sh} and P_{Lg} are the values of P for the single-component SAMs. When plotted against log R_{soln}, P has the form of a sigmoid, with its midpoint centered at $R_{soln} = 1/A$ (eq 12).

$$P_{SAM} = P_{Sh} + (P_{Lg} - P_{Sh})\left(\frac{1}{10^{-\log(AR_{soln})} + 1}\right) \quad (12)$$

In Figures 2–5, we have included a reference sigmoid in each of the plots of thickness as a dotted curve, centered at the value of $R_{soln}^{SAM=1}$ determined from the ellipsometric thicknesses of the mixed SAMs (i.e. $1/A = R_{soln}^{SAM=1,ellip}$). The noteworthy feature that emerges from each plot is that the transition region of the experimental curve is significantly sharper than that predicted by eq 12. The most plausible interpretation of this difference is that events forming thiolates at adjacent sites are *not* independent and that components on the surface interact.[18,20] The deviation of the experimental curve from the simple theoretical model is in the sense expected if Lg·Lg and Sh·Sh pairs are favored energetically relative to Lg·Sh

(33) In the calculation of ellipsometric thickness, we assume an index of refraction of 1.45; the indices of refraction for various molecules similar to those used in this study vary from 1.42 to 1.46: undecane (liquid), 1.42; undecanol (liquid), 1.44; undecanethiol (liquid), 1.46; octadecanethiol (solid), 1.46; and docosane (solid), 1.45. *CRC Handbook of Chemistry and Physics*, 65th ed.; Weast, R. C., Ed.; CRC Press Inc.: Boca Raton, FL, 1984. This potential variation in the refractive index affects the thickness <±1.5 Å which is less than the variation we normally observe for the SAMs of alkanethiolates on gold.[34]

(34) We generally assume that the precision of our ellipsometer for determining the thicknesses of SAMs of alkanethiolates on gold is approximately ±2 Å. For 108 measurements of thickness made on the single-component SAMs used in this study, the average standard deviation was 1.7 Å.

(35) Bartell, L. S.; Betts, J. F. *J. Phys. Chem.* **1960**, *64*, 1075–1076.

(36) Values of $1/R_{soln}^{SAM=1}$ were determined by plotting normalized data (d_{ellip}, $\cos\theta_a^{H_2O}$, $\cos\theta_r^{H_2O}$, ln Au(4f), ln [C(1s)/Au(4f)], O(1s)) against ln R_{soln} and fitting the data to a symmetric sigmoid with two parameters: $y = 1/[\exp(a(x - b)) + 1]$. This equation is similar to eq 12, but we have normalized it and added an extra parameter (a) to account for deviations from ideal mixing of the components. The fits were performed by the general curve fit function in the program KaleidaGraph (Synergy Software). From this equation, $1/R_{soln}^{SAM=1} = e^{-b}$. Using this method, all data points could be used in the determination of the values of $1/R_{soln}^{SAM=1}$.

(37) The mechanism of exchange between thiolates on the surface and thiols in solution has not been determined; we have assumed thermodynamic equilibrium in this model for the purpose of demonstrating that these SAMs do not follow an idealized model.

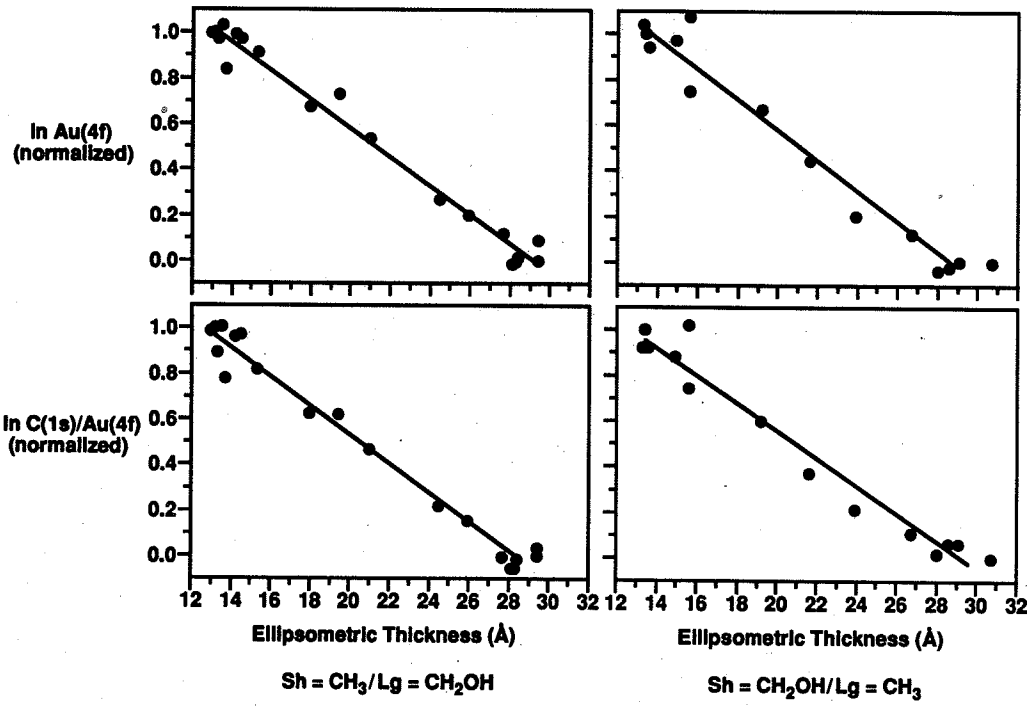

Figure 8. Plots of ln Au(4f) (top row) and ln [C(1s)/Au(4f)] (bottom row) against ellipsometric thickness for Sh = CH_3/Lg = CH_2OH (left column) and Sh = CH_2OH/Lg = CH_3 (right column). Values of ln Au(4f) and and ln [C(1s)/Au(4f)] were normalized and are therefore equal to the mole fraction of the shorter component in the SAM. Lines through the data were determined by a least-squares calculation.

pairs.[38] The displacement of $R_{soln}^{SAM=1}$ from $R_{soln} = 1$ is in the direction expected if Lg·Lg interactions are more favorable than Sh·Sh interactions (i.e. α as defined in eq 5 is negative). We note that longer times of immersion during formation of the SAMs lead to *sharper* transition regions.[27] We will therefore anticipate even sharper transitions in mixed SAMs that have been allowed to equilibrate fully with the solutions from which they were formed.

X-ray Photoelectron Spectroscopy (XPS).[39,40] Figures 2–5 present XPS data for gold, carbon, and (where useful) oxygen.[41] In quantifying individual elements using XPS, we used the 4f doublet for gold (Au(4f)[42] at 84 and 87 eV for $4f_{7/2}$ and $4f_{5/2}$, respectively) and the 1s peaks for carbon and oxygen (C(1s) and O(1s) at 284 and 532 eV, respectively).

The intensities of the gold and carbon peaks are not directly related to the compositions of the SAMs because these photoelectrons are scattered inelastically in the SAM.[43,44] The relationships between the thickness of the hydrocarbon layer of a SAM, d_{HC}, and the intensity of the photoelectrons detected for gold and carbon ($Au(4f)_{SAM}$ and $C(1s)_{SAM}$) are given in eqs 13 and 14, respectively.[43] In these equations, $Au(4f)_0$ is the intensity of the Au(4f) peaks from a bare gold substrate, β is the attenuation of the gold signal due to the sulfur atoms, $C(1s)_\infty$ is the intensity of the C(1s) peak from an infinitely thick hydrocarbon layer, λ is the attenuation length or escape depth of the photoelectrons,[43,44] and ϕ is the angle between the plane of the sample and the detector (35°).

$$Au(4f)_{SAM} = Au(4f)_0 \beta \exp(-d_{HC}/(\lambda \sin \phi)) \quad (13)$$

$$C(1s)_{SAM} = C(1s)_\infty (1 - \exp(-d_{HC}/(\lambda \sin \phi))) \quad (14)$$

Since we have not determined $Au(4f)_0$ and β, or $C(1s)_\infty$, we cannot determine the *absolute* thickness of a SAM. Using the attenuation of the Au(4f) signal, we can, however, determine the thickness of a mixed SAM *relative* to the thickness of one of the single-component SAMs. We have arbitrarily chosen to determine the thicknesses of the mixed SAMs relative to the thickness of the shorter component using eq 15 (λ = 42 Å for Au(4f))[43,44], and we present these values in Figures 2–5 beneath the thicknesses determined by ellipsometry.[45]

$$d_{SAM,XPS} - d_{Sh,XPS} = (\lambda \sin \phi) \ln (Au(4f)_{Sh}/Au(4f)_{SAM}) \quad (15)$$

(38) In a separate paper we will give a more complete experimental and theoretical description of phase separation in these SAMs including experimental conditions that will yield the most phase separated SAMs and a thermodynamic interpretation of the results (Folkers, J. P.; Laibinis, P. E.; Deutch, J. M.; Whitesides, G. M. Unpublished results).

(39) We cannot rigorously determine the error in the XPS intensities because the flux of X-rays to the sample is different for each individual run. We estimate, however, that the X-ray source (X-ray fluorescence formed by electrons from a tungsten filament striking an aluminum target) does not fluctuate more than 5% during a single set of samples.

(40) In Figures 2–5, the intensities of the carbon (1s) peaks were doubled to show the changes more clearly. Each set of XPS data was individually adjusted so that the Au(4f) intensity for the shorter component was between 6×10^5 and 7×10^5 counts.

(41) Sulfur is not included in these analyses because its peaks have low intensities relative to peaks of other elements: its elemental concentration in the SAMs is low, and photoelectrons originating in sulfur are inelastically scattered by interaction with the alkyl chains.

(42) Since we have combined the areas of the $4f_{5/2}$ and $4f_{7/2}$ peaks to give the data in Figures 2–5, we refer to these combined data simply as Au(4f).

(43) Bain, C. D.; Whitesides, G. M. *J. Phys. Chem.* **1989**, *93*, 1670–1673.

(44) Laibinis, P. E.; Bain, C. D.; Whitesides, G. M. *J. Phys. Chem.* **1991**, *95*, 7017–7021, and references therein.

(45) Ellipsometry and XPS do not give the same value for the difference in thickness between the long component and the short component. Using a refractive index of 1.45, ellipsometry gives a thickness per methylene group greater than would be expected from crystallographic data.[4] Escape depths (λ) for photoelectrons through these SAMs were determined using the crystallographic data for the alkane chains.[43,44] The error on the escape depth is approximately ±2 Å, which might also account for some of the difference observed between the thicknesses determined with these methods.

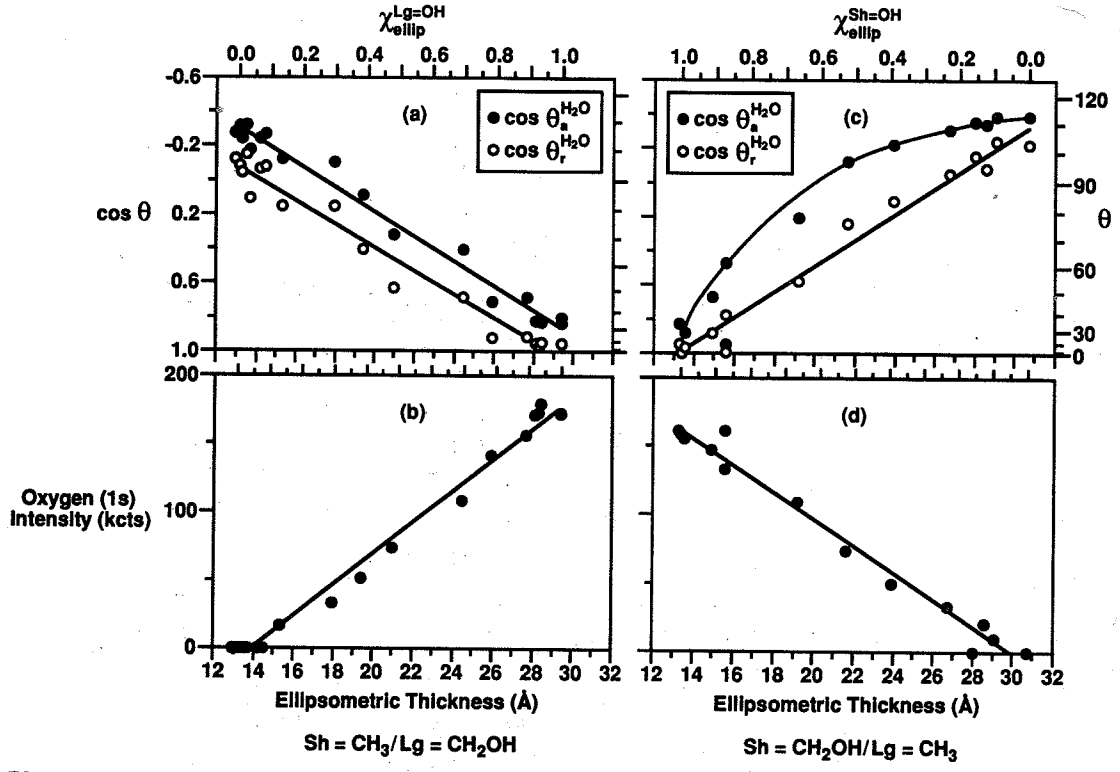

Figure 9. Plots of contact angles (top row) and oxygen (1s) XPS intensity (bottom row) against ellipsometric thickness for Sh = CH_3/Lg = CH_2OH (left column) and Sh = CH_2OH/Lg = CH_3 (right column). Straight lines were determined with a linear least-squares calculation; the curve through the advancing contact angles of water for Sh = CH_2OH/Lg = CH_3 is presented only as a guide to the eye and does not have any mathematical significance.

These thicknesses (or, more simply, ln Au(4f)$_{SAM}$) should be related linearly to the composition of the SAMs by eq 16.[46] We have also shown previously that ln [C(1s)/Au(4f)]$_{SAM}$ is related directly to the composition of a SAM (eq 17).[20,29] In Figure 8, we examine the relation between

$$\ln \mathrm{Au(4f)_{SAM}} = \chi_{Sh} \ln \mathrm{Au(4f)_{Sh}} + \chi_{Lg} \ln \mathrm{Au(4f)_{Lg}} \quad (16)$$

$$\ln [\mathrm{C(1s)/Au(4f)}]_{SAM} = \chi_{Sh} \ln [\mathrm{C(1s)/Au(4f)}]_{Sh} + \chi_{Lg} \ln [\mathrm{C(1s)/Au(4f)}]_{Lg} \quad (17)$$

ellipsometric thickness and ln Au(4f)$_{SAM}$ (eq 16) and ln [C(1s)/Au(4f)]$_{SAM}$ (eq 17) for Sh = CH_3/Lg = CH_2OH and Sh = CH_2OH/Lg = CH_3.[47] The other two systems also exhibit similar relationships, although the quality of these data is lower.[48] These linear relationships support the assumption used for eq 3. Values of $1/R_{soln}^{SAM=1}$ were also determined from these data for all four systems (Table I); these values agree well with those determined from ellipsometric thicknesses.

For mixed SAMs of Sh = CH_3/Lg = CH_2OH, the intensity of the oxygen (1s) peak should follow eq 18 provided that the hydroxymethyl terminal groups are at

$$\mathrm{O(1s)_{SAM}} = \chi_{Lg}\, \mathrm{O(1s)_{Lg}} \quad (18)$$

or near the monolayer–air interface *at all values* of R_{SAM}. In this circumstance, eq 18 need not contain a term for inelastic scattering of the oxygen photoelectrons. Figure 9b confirms that eq 18 is followed experimentally: The relation between ellipsometric thickness and O(1s) intensity is linear.[49] The value of $1/R_{soln}^{SAM=1}$ determined from the O(1s) intensity also agrees with the value determined by ellipsometry.

For Sh = CH_2OH/Lg = CH_3, the relation between ellipsometric thickness and O(1s) intensity is also linear (Figure 9d). If the two components were well mixed within the plane of the monolayer, we would expect that the O(1s) photoelectrons would be attenuated by the longer chains (especially at low values of χ_{Sh}). Using the difference in thickness between $HS(CH_2)_{11}OH$ and $HS(CH_2)_{21}CH_3$ determined from Au(4f) intensities and $\lambda \approx 30$ Å for O(1s),[44] the amount of attenuation, however, is not large enough to distinguish between well-mixed and islanded SAMs.

Contact Angles.[50] Water and hexadecane provide different details about the surfaces. Water has a high surface tension (γ_{LV} = 72 dyn/cm^2 at 25 °C)[51,52] which is dominated by its polar component (50 dyn/cm^2)[52] and its ability to form hydrogen bonds. Hexadecane has a much

(46) Equation 16 assumes that the two components are well mixed. If a two-component SAM were macroscopically phase separated (with islands smaller than the spot size of the X-ray beam), the Au(4f) intensity from the mixed SAM would be a weighted sum of the Au(4f) intensities from the single-component SAMs. Since the attenuation length (λ) of Au(4f) photoelectrons through the hydrocarbon layer is 42 Å,[43,44] the precision of our data does not allow us to differentiate the phase-separated and the well-mixed models. We have therefore chosen to use the well-mixed model because we do not have an estimate of the size of the islands in our monolayers.

(47) We have normalized these data for ease of presentation. Due to fluctuations in the intensity of the X-ray source (usually less than ~5%), some normalized data points may be less than zero or greater than one.

(48) For Sh = CH_3/Lg = CH_3 and Sh = CH_2OH/Lg = CH_2OH, the data were best fit by straight lines (note the agreement between $1/R_{soln}^{SAM=1}$ values determined by ln Au(4f)$_{SAM}$ and ln [C(1s)/Au(4f)]$_{SAM}$ and those determined by ellipsometry in Table I), but the scatter of the data was much greater than for the other two systems.

(49) For clarity in presentation, we have normalized the oxygen (1s) intensity in Figure 9 to its intensity from the single-component SAM with the hydroxymethyl tail group (i.e. O(1s)$_{Lg}$ for Sh = CH_3/Lg = CH_2OH and O(1s)$_{Sh}$ for Sh = CH_2OH/Lg = CH_3).

(50) Wetting data are plotted as the cosine of the contact angle rather than the contact angle because cos θ is related to the surface free energy through Young's equation (Young, T. *Philos. Trans. R. Soc. (London)* **1805**, *95*, 65–87).

(51) Jasper, J. J. *J. Phys. Chem. Ref. Data* **1972**, *1*, 841–1009.

(52) Cognard, J. *J. Chim. Phys.* **1987**, *84*, 357–362, and references therein.

lower surface tension (γ_{LV} = 27 dyn/cm² at 25 °C) which is entirely dispersive in origin.[51,52] Changes in the contact angles of water and hexadecane, therefore, provide information on the polar and nonpolar changes at the monolayer–liquid interface, respectively.

Water.[53] When both tail groups are the same, the contact angles of water are affected by the value of R_{SAM} but are not related to the composition of the SAMs by an equation of the form of eq 8. For Sh = CH_3/Lg = CH_3, all advancing contact angles of water for the mixed SAMs are essentially the same as those for the pure SAMs—the mixed SAMs are as hydrophobic as the pure SAMs. Receding contact angles decrease to a minimum near R_{SAM} = 1 (Figure 2): We observe repeatedly that the receding contact angles seem to be more sensitive to disorder in the SAMs than the advancing angles, but we do not presently have a rationalization for this phenomenon.

For Sh = CH_2OH/Lg = CH_2OH, both pure SAMs are hydrophilic, but the mixed SAMs are substantially more hydrophobic. The advancing contact angle of water reaches a maximum value ($\theta_{a,max}^{H_2O} \approx 54°$) near R_{SAM} = 1 (see Figure 5). This value is higher than that observed previously for SAMs derived from mixtures of $HS(CH_2)_{11}OH$ and $HS(CH_2)_{19}OH$ ($\theta_{a,max}^{H_2O} \approx 41°$),[19,20] but its origin is the same: Disorder of the type shown in region 2 of Figure 1 exposes methylene groups to the contacting water.[19,20]

In the other two systems (Sh = CH_3/Lg = CH_2OH and Sh = CH_2OH/Lg = CH_3), the contact angle of water changes smoothly between hydrophobic and hydrophilic extremes (Figures 3 and 4). These transitions are qualitatively similar to the transitions in ellipsometric thickness. Figure 9 relates the composition of the SAM (as determined from ellipsometric thickness) to cos θ^{H_2O}. We have also determined values of $1/R_{soln}^{SAM=1}$ from the advancing and receding contact angles of water for both of these systems (Table I).

For Sh = CH_3/Lg = CH_2OH (Figure 9a), both cos $\theta_a^{H_2O}$ and cos $\theta_r^{H_2O}$—within the experimental precision of our measurements—are linearly related to the composition of the SAMs (eqs 19 and 20).[54,55] The values of

$$\cos\theta_{a,surf}^{H_2O} = \chi_{Sh}\cos\theta_{a,Sh}^{H_2O} + \chi_{Lg}\cos\theta_{a,Lg}^{H_2O} \quad (19)$$

$$\cos\theta_{r,surf}^{H_2O} = \chi_{Sh}\cos\theta_{r,Sh}^{H_2O} + \chi_{Lg}\cos\theta_{r,Lg}^{H_2O} \quad (20)$$

$1/R_{soln}^{SAM=1}$ determined using both cos $\theta_a^{H_2O}$ and cos $\theta_r^{H_2O}$ agree with values determined by other methods (see Table I).

For Sh = CH_2OH/Lg = CH_3, the situation is considerably different. Only the receding contact angles of water are directly related to the composition of the SAMs (eq 20, Figure 9c; also see Table I). The plot of advancing contact angle of water against ellipsometric thickness is curved (Figure 9c) and yields a value of $1/R_{soln}^{SAM=1}$ larger than the other values (Table I). We suggest that the behavior of this system may reflect time-dependent restructuring of the interfaces: In contact with air, the interface minimizes the solid–vapor interfacial tension γ_{SV} by maximizing the number of exposed CH_3 and CH_2 groups; in contact with water, the interface minimizes the solid–liquid interfacial tension γ_{SL} by maximizing the number of exposed CH_2OH groups and minimizing the number of exposed CH_3 and CH_2 groups.[56]

Hexadecane.[57,58] The advancing contact angles of hexadecane on mixed SAMs with at least Sh or Lg = CH_3 present a self-consistent picture of the sensitivity of hexadecane to the components in these SAMs. For Sh = CH_3/Lg = CH_3, θ_a^{HD} quickly decreases from $\theta_{a,Sh}^{HD}$ to a minimum near χ_{Lg} = 0.2 ($\theta_{a,min}^{HD}$ = 16°) and then slowly increases up to $\theta_{a,Lg}^{HD}$ (Figure 10b). This decrease corresponds to the expected change as the SAM progresses from an ordered, low-energy surface composed of CH_3 groups through a higher energy and more disordered phase, back to an ordered phase exposing primarily CH_3 groups. For Sh = CH_2OH/Lg = CH_3, θ_a^{HD} increases linearly with the amount of the longer component in the SAM. This behavior mimics the shape of the curve for Sh = CH_3/Lg = CH_3 for $\chi_{Lg} > 0.2$ (Figure 10a).[60] For Sh = CH_3/Lg = CH_2OH, θ_a^{HD} decreases to near zero for $\chi_{Lg} < 0.1$ (Figure 10c); this curve is similar to that for Sh = CH_3/Lg = CH_3 when $\chi_{Lg} < 0.2$. These results suggest that the advancing contact angle of hexadecane is most sensitive to the lg–sh methylene chains and the tail group of longer component but is only sensitive to the tail group on the shorter component at high values of χ_{Sh} (i.e. low values of χ_{Lg}).

Hysteresis in the Contact Angle of Water.[61] Hysteresis (defined here by eq 21, and plotted in the figures as $-\Delta\cos\theta$ for convenience; a large value of hysteresis is a large value of $-\Delta\cos\theta$) between the advancing and

$$\Delta\cos\theta = \cos\theta_a - \cos\theta_r \quad (21)$$

receding contact angles of water is largest for all systems when the interface between the SAM and the contacting liquid is most disordered.[62] Error bars for hysteresis were determined from the average errors in cos $\theta_a^{H_2O}$ and cos $\theta_r^{H_2O}$ for

(53) In these studies, the precision of the contact angles of water was approximately ±3°, corresponding to errors in cos θ between 0.03 and 0.05. Error bars in Figures 2–5 represent the average error in cos θ for the contact angles in the transition region for each separate system; approximately 100 values were used to determine these error bars for each individual system. The errors in the advancing and receding contact angles were determined separately. For Sh = CH_2OH/Lg = CH_2OH, the error bars are smaller than the size of the symbols.

(54) Equations 19 and 20 are similar in form to Cassie's relation (Cassie, A. B. D. *Discuss. Faraday Soc.* **1948**, *3*, 11–16); Cassie's relation is, however, defined for equilibrium contact angles on surfaces with fractional areas of different wettabilities. We do not refer to eqs 19 and 20 as "Cassie's" relations because we do not know the relationship between the mole fraction of the longer component in the SAM and its fractional area in the monolayer–liquid or monolayer–air interface. This relationship would depend on the difference in chain length and the degree of islanding in the SAM.

(55) Since we do observe an increase in the hysteresis in the contact angle of water on mixed SAMs of Sh = CH_3/Lg = CH_2OH, one or both of either cos $\theta_a^{H_2O}$ or cos $\theta_r^{H_2O}$ must not be related linearly to the composition of the SAM, but within the precision of the data taken in this study, we cannot determine which it is since both sets of data can be fit to straight lines with similar accuracies.

(56) From Young's equation,[50] γ_{XY} is the interfacial free energy between the two phases X and Y. Abbreviations for the phases are S = solid (SAM), L = liquid (water or hexadecane), and V = vapor (ambient laboratory atmosphere).

(57) Error bars for these contact angles are smaller than the size of the symbols.

(58) Because the length of hexadecane (16 carbons) is significantly greater than lg – sh (11 carbons), shape-selective interactions[20,59] between hexadecane and the mixed SAMs probably do not affect the contact angles of hexadecane.

(59) Bartell, L. S.; Ruch, R. J. *J. Phys. Chem.* **1956**, *60*, 1231–1234. Bartell, L. S.; Ruch, R. J. *J. Phys. Chem.* **1959**, *63*, 1045–1048.

(60) From these data, $1/R_{soln}^{SAM=1}$ = 8, which is in the range of the other values for this system (see Table I for the other values).

(61) When the receding angle is zero, values of hysteresis are not plotted. Similarly, the hysteresis in the contact angle of hexadecane is not included because there are not enough usable data points from which to draw conclusions.

(62) Theoretical investigations on the origins of hysteresis have not addressed hysteresis on surfaces that are heterogeneous on a molecular level. See, for example: Joanny, J. F.; de Gennes, P. G. *J. Chem. Phys.* **1984**, *81*, 552–562. Schwartz, L. W.; Garoff, S. *Langmuir*, **1985**, *1*, 219–230. de Gennes, P. G. *Rev. Mod. Phys.* **1985**, *57*, 827–863.

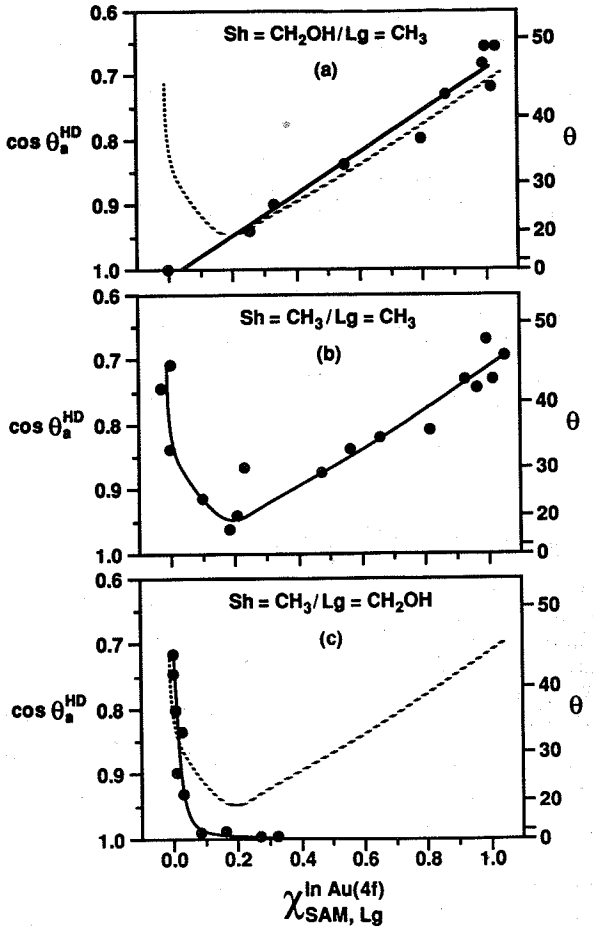

Figure 10. Plots of the advancing contact angle of hexadecane against the mole fraction of the longer component in the SAM as determined from ln Au(4f) for (a) Sh = CH_2OH/Lg = CH_3, (b) Sh = CH_3/Lg = CH_3, and (c) Sh = CH_3/Lg = CH_2OH. The solid line in part a was determined with linear least-squares calculation; the solid lines in parts b and c are only drawn as guides to the eye and have no mathematical significance. For reference, parts a and c include the line in part b as a dashed line.

the transition regions of the individual systems; relatively small errors in cos θ_a and cos θ_r lead to a relatively large error in Δ cos θ. The magnitude of this error may also reflect differences in the roughness of the substrates from experiment to experiment or sample to sample.[62]

Discussion

Ellipsometry and XPS Provide Complementary Techniques for Determining the Composition of Mixed SAMs. The use of optical ellipsometry to determine the composition of mixed SAMs requires that the two components separately form SAMs with significantly different thicknesses and that mixtures of the two components form SAMs in which the thickness can be linearly related to the composition (i.e. the refractive index for all SAMs is approximately the same regardless of R_{SAM}). Three types of XPS measurements provide independent checks on the relation between the measured thickness and composition of the SAMs and yield data in good agreement with ellipsometry: (i) the absolute attenuation of the Au(4f) signal (eq 13) gives a measure of the thickness of a mixed SAM relative to the thickness of a SAM having a single component (eq 15); (ii) the logarithm of the ratio of C(1s) to Au(4f) is related to the composition of the SAMs (eq 17);[20] (iii) the intensity of the signal from a unique element in an appropriate sample (e.g. O(1s) in Sh = CH_3/Lg = CH_2OH, but not necessarily in Sh = CH_2OH/Lg = CH_3) provides another measure of composition of the SAMs (eq 18).

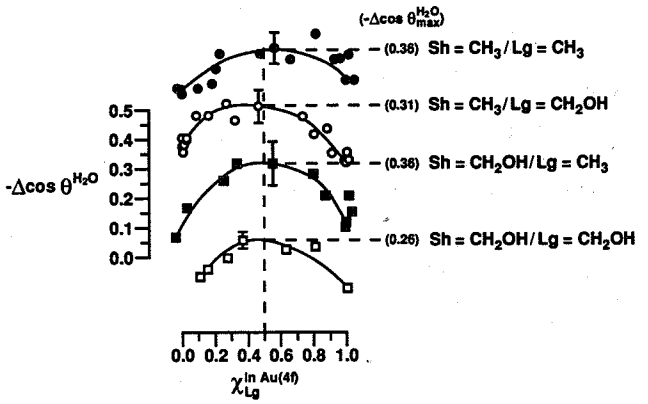

Figure 11. Plot of hysteresis against the mole fraction of the longer component in the SAM as determined from the values of ln Au(4f). Data sets were offset vertically by 0.55, 0.40, 0.15, and 0.0 for Sh = CH_3/Lg = CH_3, Sh = CH_3/Lg = CH_2OH, Sh = CH_2OH/Lg = CH_3, and Sh = CH_2OH/Lg = CH_2OH, respectively. Error bars were determined from the average error bar in cos $\theta_a^{H_2O}$ and cos $\theta_r^{H_2O}$ and are representative for the transition region.[53] The numbers in parentheses correspond to the maximum values of hysteresis for that system. For Sh = CH_3/Lg = CH_3, Δ cos θ_{max} = 0.36 at χ_{Lg} = 0.57 (Δ cos θ = 0.41 at χ_{Lg} = 0.81); for Sh = CH_3/Lg = CH_2OH, Δ cos θ_{max} = 0.32, 0.31 at χ_{Lg} = 0.27, 0.54, respectively; for Sh = CH_2OH/Lg = CH_3, Δ cos θ_{max} = 0.37, 0.36 at χ_{Lg} = 0.33, 0.55, respectively; and for Sh = CH_2OH/Lg = CH_2OH, Δ cos θ_{max} = 0.26 at χ_{Lg} = 0.37. Since the value of Δ cos θ at $\chi \approx 0.8$ for Sh = CH_3/Lg = CH_3 does not fit the general trend of the data, we have not used it as Δ cos θ_{max}. Two values of Δ cos θ_{max} are listed above for Sh = CH_3/Lg = CH_2OH and Sh = CH_2OH/Lg = CH_3 because these two values differed by only 0.01; the lines in the figures are drawn to the data point closest to χ = 0.5, and this value of hysteresis is listed in parentheses in the figure.

We increasingly use XPS data in preference to ellipsometry to establish the composition of SAMs, for several reasons. First, the precision of XPS intensities (usually better than ±5%) is greater than the precision of ellipsometric thicknesses for SAMs of alkanethiolates on gold (approximately ~10–15% or ±~2 Å). Since calculation of ellipsometric thicknesses requires the optical constants of the bare substrate and the functionalized substrate, these thicknesses are affected by the physisorption of contaminants onto the gold prior to formation of the SAM.[5,63] Because these contaminants are removed from the gold during formation of the SAM,[5] XPS intensities are not affected. Second, the attenuation of the photoelectrons from the substrate can provide the thickness of a mixed SAM relative to a standard, alleviating the need for ellipsometry to determine thickness.[43,44,64] Third, XPS provides chemical information about the SAMs (e.g. oxidation state of the sulfur;[14] the presence of any potential contaminants in the gold) at the same time that it measures thickness.

Because ellipsometry yields an absolute thickness, it is still a convenient method for determining the composition of a mixed SAM. The method is less time consuming and expensive than XPS[65] and does not require relating the results to a standard. When only a rough estimate of

(63) The initial optical constants of the bare gold substrates display greater variation per sample than the constants after formation of the SAM. This observation suggests that adsorbates present on the substrates are removed from the surface of the gold during formation of the SAM.

(64) Absolute thicknesses of SAMs can be determined from XPS by comparing the intensity of the Au(4f) photoelectrons from a SAM to that of a piece of gold that had been sputtered clean inside the XPS using an argon sputterer.

composition for one mixed SAM is needed, ellipsometry is probably the method of choice, but XPS is much better for determining surface composition for an entire set of SAMs.

Contact Angle of Water Can Also Provide an Estimate of the Composition of a Mixed SAM. In the systems with only one terminal hydroxymethyl group (Sh = CH_3/Lg = CH_2OH or Sh = CH_2OH/Lg = CH_3), the contact angle of water is also a convenient method for determining the composition of mixed SAMs. For Sh = CH_3/Lg = CH_2OH, the advancing angle is probably most convenient for determining the composition of a mixed SAM. Since we do not have a theoretical model to explain the linear behavior observed in these systems, we cannot recommend this method for determining the composition of a new mixed SAM, until the method has been calibrated by some better understood technique.

Wetting: Disorder in the SAM Can Increase or Decrease Its Wettability Depending on the Components in the SAM and the Contacting Liquid. The relation between cos θ and the composition on the surface in mixed SAMs demonstrates both the complexity of the interactions between the monolayer–air interface and the probe liquid at molecular scales, and the utility of these SAMs in exploring wetting. SAMs having the same terminal group on both components (Sh = CH_3/Lg = CH_3 or Sh = CH_2OH/Lg = CH_2OH) show significant differences in wettability for disordered, mixed surface phases and ordered, single-component phases, but the character of this difference depends on the system. The system of Sh = CH_3/Lg = CH_3 shows a large *increase* in wettability by hexadecane at $R_{SAM} \approx 0.25$ (cos θ_a^{HD} changes by approximately 0.25; this value corresponds to an increase in interfacial free energy, $\gamma_{SV}-\gamma_{SL}$,[56] of approximately 0.2 kcal/mol of "surface groups"[66]). The advancing contact angle of water is, however, unaffected by formation of this mixed phase, but the receding angle decreases, and the hysteresis in contact angles correspondingly increases. The system of Sh = CH_2OH/Lg = CH_2OH shows a significant *decrease* in wettability by water near $R_{SAM} = 1$ (cos $\theta_a^{H_2O}$ changes by approximately 0.35; 0.8 kcal/mol).[66] Each of these observations (with the exception of the behavior of $\theta_r^{H_2O}$ for Sh = CH_3/Lg = CH_3) can be rationalized by using models of the type suggested by Figure 12.

The behavior of the contact angle of water on mixed SAMs with different terminal groups (Sh = CH_3/Lg = CH_2OH and Sh = CH_2OH/Lg = CH_3) shows a qualitatively satisfying correlation between hydrophilicity and content of hydroxyl groups (Figure 9), with both systems ranging from nearly wettable ($\theta_a^{H_2O} < 30°$) to very hydrophobic ($\theta_a^{H_2O} > 110°$). Closer analysis of these data suggests greater complexity: For Sh = CH_3/Lg = CH_2OH both cos $\theta_a^{H_2O}$ and cos $\theta_r^{H_2O}$ are linearly related to χ_{OH}, the mole fraction of the hydroxymethyl-terminated species on the surface, within the experimental error of the measurements involved.[55] For Sh = CH_2OH/Lg = CH_3, cos $\theta_r^{H_2O}$ is linear in χ_{OH} (as determined from ellipsometry, Figure 9), while cos $\theta_a^{H_2O}$ is strongly curved as a function of χ_{OH}. What is the difference in these systems? We can only hypothesize

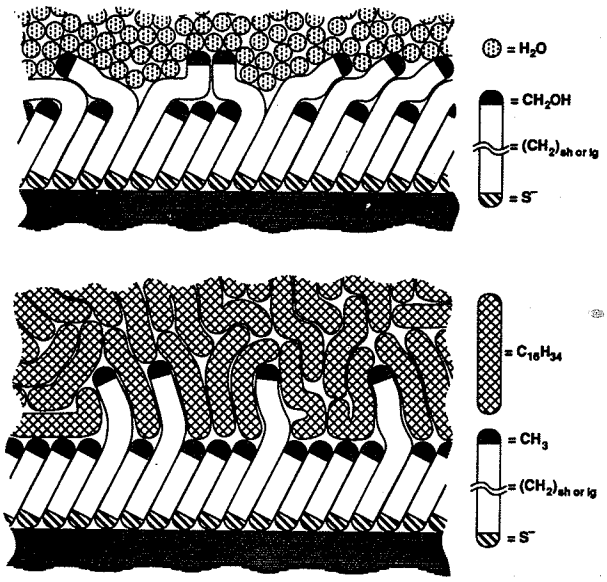

Figure 12. Schematic representation of a mixed SAM derived from Sh = CH_2OH/Lg = CH_2OH in contact with water (top) and of mixed SAM derived from Sh = CH_3/Lg = CH_3 in contact with hexadecane (bottom). Only several layers of solvent molecules above the SAM are represented, and these only schematically. The compositions of the SAMs in these figures are those at which the wettability has changed the most from the values of the single-component SAMs. In the case of Sh = CH_2OH/Lg = CH_2OH, $\theta_a^{H_2O} = 52°$ for $R_{SAM} = 1$; in the case of Sh = CH_3/Lg = CH_3, $\theta_a^{HD} = 16°$ for $R_{SAM} = 0.25$.

that Sh = CH_3/Lg = CH_2OH has the hydroxyl groups available in the outer part of the SAM and accessible at all times to the drop of water; in Sh = CH_2OH/Lg = CH_3 the hydroxyl groups are partially buried in the SAM, and achieving optimal interaction with water requires a relatively slow reorganization of the surface. This reorganization may only be fully reflected in interfacial free energies as the drop recedes. We have no direct evidence supporting this hypothesis, but the advancing contact angle of hexadecane on mixed SAMs of Sh = CH_2OH/Lg = CH_3 is also consistent with a hypothesis suggesting that wetting should be relatively insensitive to the tail groups on the shorter components of a mixed SAM.

R_{SAM} in Mixed SAMs Depends on Both the Concentrations and the Structures of the Thiols in Solution. Two important conclusions concerning the adsorption of these thiols onto gold from the experiments described here are that (i) R_{SAM} differs from R_{soln} in the direction indicating a preference for inclusion of longer chain thiolates in the SAM[18-20] and (ii) the shape of the curve of χ_{SAM} (designated by ellipsometric thickness) vs R_{soln} suggests significant interactions between adjacent sites favoring Lg·Lg and Sh·Sh pairs relative to Lg·Sh pairs.[18,20,38] The tail group of the longer thiol has an effect on the relationship between R_{SAM} and R_{soln} (see Table I); differences in the solvation of the tail groups by ethanol are significant and are probably the major cause of this difference.[17,20]

Are the Components of Mixed SAMs Phase Separating into Islands?[18-20] We have two independent types of information that bear on this question. One can be explained only if there is significant mixing of the components and the other only if there is significant phase separation. From these divergent conclusions, we hypothesize that the mixed SAMs studied here exist in a state intermediate between completely mixed and fully phase separated. We know from studies of mixed SAMs prepared under different experimental conditions (longer

(65) Ellipsometry may also be more useful for determining the compositions of Langmuir–Blodgett films or different self-assembled monolayers that might be only weakly adsorbed to the surface because the ultrahigh vacuum required for XPS could cause desorption of volatile adsorbates.

(66) In the determination of the change in interfacial energy with change in contact angle, we used an area per surface group in the SAM of 21.65 Å²/molecule. The experimentally determined distance between hexagonally packed alkanethiolates on gold(111) is 5.0 Å.[6,7,13]

and shorter adsorption times, more concentrated and more dilute solutions of thiols, higher and lower temperatures)[27] that the extent of mixing can be changed.[38] We sketch here the relevant information leading to the hypothesis of a kinetically determined intermediate degree of mixing/phase separation but defer a detailed discussion until additional studies are complete.

The dependence of wettability on the composition in mixed SAMs of Sh = CH_2OH/Lg = CH_2OH and Sh = CH_3/Lg = CH_3 requires some mixing. The most compelling evidence for mixing is given in the plots of cos θ vs R_{soln} in Figures 5 and 2, respectively. If mixed SAMs comprising Sh = CH_2OH/Lg = CH_2OH were macroscopically phase separated, their wettability by water would be nearly independent of R_{SAM}: the local structures of the separated phases should be approximately the same as that of the pure phases. The pure phases separately have very similar wettabilities. A mixture of islands of the pure phases should thus behave very similarly to a single, pure phase, until the islands become so small that disorder at their borders becomes significant in determining the macroscopic interfacial free energy. The pronounced increase in hydrophobicity at $R_{SAM} \approx 1$ ($R_{soln} \approx 0.2$) strongly suggests exposure of methylene groups in a disordered, mixed phase. We cannot, however, estimate the *extent* of mixing from these data, since we do not presently have data from an authentic, completely mixed system. The data for wetting of mixed SAMs of Sh = CH_3/Lg = CH_3 by hexadecane are best explained in the same way: The significant increase in wettability in this system at $R_{SAM} \approx 0.25$ ($R_{soln} \approx 0.05$) reflects interaction of a disordered, solvent-swollen mixed phase with solvent.

The dependence of R_{SAM} on R_{soln} indicates cooperativity and suggests phase separation. The composition of the SAMs is given by R_{SAM} (eq 2) and inferred experimentally from the properties of the SAMs. The deviation between the experimental values of thickness (and thus R_{SAM}) and the values calculated assuming independence of sites (Figures 2–5, dotted curves; eq 12) indicate significant interaction between adjacent methylene chains, and is in the sense expected for a phase separated system.

From these data we infer that phase separation occurs in these mixed SAMs, but that it is not complete. Phase separation in organic monolayer systems that are mobile in the plane of the monolayer (namely Langmuir films) is, of course, well-known.[67,68]

Conclusions

The data summarized in this paper illustrate several important points about self-assembled monolayers of alkanethiolates on gold. First, it is incorrect to assume that the composition of the SAM is equal to the composition of the solution. With the methodology described in this paper, SAMs can, however, be prepared reliably with known compositions. Second, the composition of the SAM can be determined by a variety techniques, of which we believe that X-ray photoelectron spectroscopy provides the most reliable values. In the systems we have studied here, ellipsometry and contact angles can also provide reliable measures of the composition of the SAMs but do not provide the range of complementary types of information that XPS does. Third, the wetting properties of the mixed SAMs strongly depend on the tail groups of the components, the difference in the chain length between the two components, and the ratio of the two components on the surface. The studies of wetting show that contact angles and the hysteresis between the advancing and the receding contact angles depend strongly on the angstrom-level structure of the surface. Fourth, the components in the mixed SAMs are not randomly dispersed on the surface. Similar molecules appear to aggregate in the SAMs; wetting studies suggest that islands are not macroscopically large.

Other details of these systems await further study: determination of the size of islands within the SAMs, determination of the mechanisms of adsorption and exchange, and separation of the kinetic and thermodynamic factors that determine the composition of these mixed SAMs.[27,38] The morphology of the gold surface may be an important factor in determining the composition of these SAMs. Exchange studies on polycrystalline gold have implied that exchange is initially dominated by defects sites on the surface[32] and that exchange in closed-packed regions of the SAM is slower than that in the disordered regions. The amount of exchange may be different on substrates with less corrugation than those used in these studies (see Figure 7). The results in this paper can be reproducibly used for the functionalization of routinely evaporated gold but may not be directly applicable for annealed, flat gold surfaces.[31]

Experimental Section

Materials. Absolute ethanol (Quantum Chemical Corp.) was deoxygenated with N_2 or Ar prior to use. Hexadecane (Aldrich, 99%) was percolated twice through activated, neutral alumina (EM Science). Water was deionized and distilled in a glass and Teflon apparatus. Undecanethiol (Pfaltz & Bauer) was distilled prior to use. Docosanethiol,[5] 11-mercaptoundecanol,[5] and 22-mercaptodocosanol[24] were available from previous studies.

Substrate Preparation. Gold substrates were prepared by electron-beam evaporation of ~2000 Å of gold (Materials Research Corp., Orangeburg, NY; 99.999%) onto single-crystal silicon (100) test wafers (Monsanto, MEMC, and Silicon Sense, Nashua, NH; 100 mm diameter, ~500 μm thick) that had been precoated with 100–200 Å of chromium (Johnson Mathey, 99.997%; Aldrich, >99.99%) as an adhesion promotion layer between the silicon dioxide and the gold. The substrates were stored in wafer holders (Fluoroware) until used in experiments. Before being added to solutions, the gold-coated silicon wafers were cut into ~1 cm × 3 cm slides with a diamond-tipped stylus, rinsed with ethanol, and blown dry in a stream of nitrogen. The time between removal of the wafers from the evaporator and addition to solution was generally less than 4 h.

Monolayer Formation. Adsorptions were carried out in 25-mL glass weighing bottles that had been cleaned with "piranha solution" (7:3 concentrated H_2SO_4/30% H_2O_2) at 90 °C for 1 h, and rinsed first with distilled water and then with copious amounts of deionized water. **WARNING:** *Piranha solution should be handled with caution. It should not be allowed to contact significant quantities of oxidizable organic materials. In some circumstances (most probably when mixed with significant quantities of an oxidizable organic material), it has detonated unexpectedly.*[69] The weighing bottles were stored in

(67) Distinct phases within Langmuir monolayers have been observed directly with the use of the epifluorescence microscope: Von Tscharner, V.; McConnell, H. M. *Biophys. J.* **1981**, *36*, 409–419. Lösche, M.; Sackmann, E.; Möhwald, H. *Ber. Bunsen-Ges. Phys. Chem.* **1983**, *87*, 848–852. McConnell, H. M.; Tamm, L. K.; Weis, R. M. *Proc. Natl. Acad. Sci. U.S.A.* **1984**, *81*, 3249–3253. Weis, R. M.; McConnell, H. M. *Nature (London)* **1984**, *310*, 47–49. Heckl, W. M.; Möhwald, H. *Ber. Bunsen-Ges. Phys. Chem.* **1986**, *90*, 3249–3253.

(68) Phase separation has been observed for Langmuir films containing a phosphatidylcholine and a small mole fraction of cholesterol; for examples, see: Pagano, R. E.; Gershfeld, N. L. *J. Phys. Chem.* **1972**, *76*, 1238–1243. Gershfeld, N. L.; Pagano, R. E. *J. Phys. Chem.* **1972**, *76*, 1244–1249. Subramaniam, S.; McConnell, H. M. *J. Phys. Chem.* **1987**, *91*, 1715–1719. Heckl, W. M.; Cadenhead, D. A.; Möhwald, H. *Langmuir*, **1988**, *4*, 1352–1358.

(69) Several warnings have recently appeared concerning "piranha solution": Dobbs, D. A.; Bergman, R. G.; Theopold, K. H. *Chem. Eng. News* **1990**, *68*(17), 2. Wnuk, T. *Chem. Eng. News* **1990**, *68*(26), 2. Matlow, S. L. *Chem. Eng. News* **1990**, *68*(30), 2.

an oven at approximately 200 °C until use. Adsorptions were carried out in 25 mL of deoxygenated ethanol at a total concentration of thiol of 1 mM. All adsorptions were performed at room temperature for 1 day.

Instrumentation. Ellipsometric measurements were performed on a Rudolf Research Type 43603-200E ellipsometer equipped with a He–Ne laser (λ = 6328 Å) at an incident angle of 70°. Samples were rinsed with ethanol and blown dry in a stream of nitrogen prior to characterization. Values of thickness were calculated using a program written by Wasserman,[70] following an algorithm by McCrackin and co-workers;[71] in the calculation, we used a refractive index of 1.45 for the SAMs.[33]

Contact angles were measured on a Ramé-Hart Model 100 goniometer at room temperature and ambient humidity for both water and hexadecane. Advancing and receding contact angles were measured on both sides each of at least 3 drops of each liquid per slide; data in the figures represent the average of these measurements. A Micro-Electrapette syringe (Matrix Technologies: Lowell, MA) was used for dispensing/removing the liquids onto/from the SAMs (~1 μL/s). The method used for measuring the advancing and receding angles has been described previously.[5] XPS was carried out using an SSX-100 spectrometer (Surface Science Instruments) using monochromatic Al Kα X-rays (λ = 8.3 Å). The spot size for all spectra was 1 mm, with a pass energy on the detector of 100 eV. Two scans were taken for both gold and carbon, and five scans were taken for oxygen (acquisition time for one scan at this resolution was approximately 2 min). Spectra were fitted using a 80% Gaussian/20% Lorentzian function in the computer system of the SSX-100.

The gold sample used for microscopy had 250 Å of chromium as an adhesive layer followed by 2000 Å of gold. The scanning electron micrograph in Figure 6 was taken on a JEOL JSM-6400 scanning electron microscope with an accelerating voltage of 20 kV. The scanning tunneling microscope used for the images in Figure 7 was a Nanoscope II operated in constant height mode with a bias voltage of −164.5 mV.

Acknowledgment. We thank Bob Graham and Yuan Lu for the scanning electron micrographs. Our colleagues Yun Kim and Charles M. Lieber provided the scanning tunneling micrographs of our gold samples. We thank Hans Biebuyck, Kevin Prime, and Greg Ferguson for useful discussions. We also thank H.B. for invaluable technical assistance.

Registry No. Au, 7440-57-5; $HS(CH_2)_{10}CH_3$, 5332-52-5; $HS(CH_2)_{10}CH_2OH$, 73768-94-2; $HS(CH_2)_{21}CH_3$, 7773-83-3; $HS(CH_2)_{21}CH_2OH$, 137057-24-0; hexadecane, 544-76-3.

(70) Wasserman, S. R. Ph.D. Thesis, Harvard University, 1989.
(71) McCrackin, F. L.; Passaglia, E.; Stromberg, R. R.; Steinberg, H. L. *J. Res. Natl. Bur. Stand., Sect. A* **1963**, *67*, 363–377.